

# Changes in extracellular space size and geometry in APP23 transgenic mice: A model of Alzheimer's disease

Eva Syková<sup>\*†‡</sup>, Ivan Voříšek<sup>\*†</sup>, Tatiana Antonova<sup>\*†</sup>, Tomáš Mazel<sup>\*†</sup>, Melanie Meyer-Luehmann<sup>§</sup>, Mathias Jucker<sup>§</sup>, Milan Hájek<sup>†¶</sup>, Michael Or<sup>¶\*\*</sup>, and Jan Bureš<sup>||</sup>

<sup>\*</sup>Institute of Experimental Medicine, Academy of Sciences of the Czech Republic, Vídeňská 1083, 142 20 Prague 4, Czech Republic; <sup>†</sup>Department of Neuroscience and Center for Cell Therapy and Tissue Repair, Charles University, Second Medical Faculty, Vúvalu 84, 150 06 Prague 5, Czech Republic; <sup>§</sup>Department of Cellular Neurology, Hertie Institute for Clinical Brain Research, University of Tübingen, Otfried-Müller Strasse 27, D-72076 Tübingen, Germany; <sup>¶</sup>Department of Radiology, Institute for Clinical and Experimental Medicine, Vídeňská 1958, 140 21 Prague 4, Czech Republic; <sup>||</sup>Institute of Physiology, Academy of Sciences of the Czech Republic, Vídeňská 1083, 142 20 Prague 4, Czech Republic; and <sup>\*\*</sup>Department of Psychiatry, Charles University, First Medical Faculty, Ke Karlovu 2, 128 08 Prague 2, Czech Republic

Contributed by Jan Bureš, November 21, 2004

**Diffusion parameters of the extracellular space (ECS) are changed in many brain pathologies, disturbing synaptic as well as extrasynaptic "volume" transmission, which is based on the diffusion of neuroactive substances in the ECS. Amyloid deposition, neuronal loss, and disturbed synaptic transmission are considered to be the main causes of Alzheimer's disease dementia. We studied diffusion parameters in the cerebral cortex of transgenic APP23 mice, which develop a pathology similar to Alzheimer's disease. The real-time tetramethylammonium (TMA) method and diffusion-weighted MRI were used to measure the ECS volume fraction ( $\alpha$  = ECS volume/total tissue volume) and the apparent diffusion coefficients (ADCs) of TMA ( $ADC_{TMA}$ ), diffusing exclusively in the ECS and of water ( $ADC_W$ ). Measurements were performed *in vivo* in 6-, 8-, and 17- to 25-month-old hemizygous APP23 male and female mice and age-matched controls. In all 6- to 8-month-old APP23 mice, the mean ECS volume fraction,  $ADC_{TMA}$ , and  $ADC_W$  were not significantly different from age-matched controls ( $\alpha = 0.20 \pm 0.01$ ;  $ADC_{TMA}$ ,  $580 \pm 16 \mu m^2 s^{-1}$ ;  $ADC_W$ ,  $618 \pm 19 \mu m^2 s^{-1}$ ). Aging in 17- to 25-month-old controls was accompanied by a decrease in ECS volume fraction and  $ADC_W$ , significantly greater in females than in males, but no changes in  $ADC_{TMA}$ . ECS volume fraction increased ( $0.22 \pm 0.01$ ) and  $ADC_{TMA}$  decreased ( $560 \pm 7 \mu m^2 s^{-1}$ ) in aged APP23 mice. The impaired navigation observed in these animals in the Morris water maze correlated with their plaque load, which was twice as high in females (20%) as in males (10%) and may, together with changed ECS diffusion properties, account for the impaired extrasynaptic transmission and spatial cognition observed in old transgenic females.**

aging | cortex | diffusion | ion-selective microelectrodes | magnetic resonance

**A**lzheimer's disease is the most common form of cerebral degeneration leading to dementia. A key neuropathological feature of Alzheimer's disease is the deposition of amyloid fibrils within the neuropil as senile plaques and in the walls of cerebral and meningeal blood vessels (1). The major component of the extracellular amyloid deposits is a 40- to 42-residue protein [termed amyloid  $\beta$ -protein (2, 3)], which is derived from the endoproteolysis of the integral membrane amyloid precursor protein (APP) (4). Normally, rodents do not develop amyloid plaques; however, APP23 transgenic mice with neuron-specific overproduction of mutated human APP751 (Swedish double mutation) show their first amyloid plaques as early as 6 months of age (5). Recent experiments (6) revealed that amyloid plaques may also form in wild-type grafts implanted into the brain of APP23 transgenic animals, showing that the formation of  $\beta$ -amyloid plaques is possible even in the absence of the intracellular production of the amyloid protein.

The extracellular space (ECS) forms the microenvironment of cells, and its size and composition are important for their function. Neurons and glial cells release neuroactive substances, which then diffuse in the ECS to reach their target receptors (7, 8). This mode of extrasynaptic communication is called "volume" transmission (9, 10). Investigators have hypothesized that volume transmission provides a mechanism of long-term information processing in functions such as vigilance, sleep, depression, memory formation, and CNS plasticity (7, 11). Extrasynaptic transmission is strongly modulated by the ability of neurotransmitters to diffuse in the ECS (i.e., by their diffusion coefficient in the ECS) and by the space available for diffusion (i.e., the size of the ECS), which are parameters that are altered during many pathological as well as physiological states (11), including development and aging (12, 13). The common symptoms of Alzheimer's disease are forgetfulness, sleeplessness, anxiety, and depression, which are impaired functions in which extrasynaptic transmission could also be involved (10).

The aim of our study was to investigate diffusion changes in the cerebral cortex of transgenic APP23 mice, which develop amyloid plaques during aging. The extracellular diffusion parameters were studied by the real-time tetramethylammonium (TMA) method (14). This method can estimate the ECS volume fraction  $\alpha$  that describes the size of the ECS ( $\alpha$  = ECS volume/total tissue volume) and the apparent diffusion coefficient (ADC) of TMA ( $ADC_{TMA}$ ) in the ECS by monitoring the diffusion of TMA introduced into the ECS (15). Although the nonspecific loss of TMA from the ECS is very low, it is described by a third parameter: the nonspecific cellular uptake of TMA ( $k'$ ). The  $ADC_{TMA}$  in the ECS is always less than its free diffusion coefficient because of the complexity of the ECS, which introduces obstacles into the diffusion pathway of TMA (e.g., cellular structures or extracellular matrix molecules) and, thus, obstructs the diffusion of TMA as compared with a free medium. Therefore, the ADC in the ECS does not depend only on the physical properties of the diffusing compound (as is the case with the free diffusion coefficient) but also on the composition and structure of the ECS (16, 17). Although the TMA method is the only one that yields absolute values of  $\alpha$ ,  $ADC_{TMA}$ , and  $k'$ , it cannot be used in humans because of its invasiveness. This fact makes it difficult to compare TMA results obtained in APP23 mice to data obtained in Alzheimer's disease patients. To supplement our study, we used diffusion-weighted MRI (DW-MRI), which is widely available as an adjunct to MRI scanners in regular clinical use. By using DW-MRI, we measured the ADC of water ( $ADC_W$ ) in the

Abbreviations: ADC, apparent diffusion coefficient; MR, magnetic resonance; TMA, tetramethylammonium;  $ADC_{TMA}$ , ADC of TMA;  $ADC_W$ , ADC of water; ECS, extracellular space; ISM, ion-selective microelectrode; DW-MRI, diffusion-weighted MRI.

<sup>†</sup>To whom correspondence should be sent at the \* address. E-mail: sykova@biomed.cas.cz.

© 2005 by The National Academy of Sciences of the USA

tissue. Our aim was to correlate the changes in ECS diffusion parameters with the results of DW-MRI measurements, amyloid plaque load, and behavioral deficits.

## Materials and Methods

**Transgenic Mice.** The generation of APP23 transgenic mice has been described (5). Briefly, a murine Thy-1 promoter element was used to drive the neuron-specific expression of mutated human APP751 (Swedish double mutation) in B6D2 mice. Hemizygous APP23 mice (6- to 8-months old and 17- to 25-months old) and age-matched nontransgenic controls were used. The mice were from the F<sub>8</sub>-F<sub>10</sub> generations of backcrossing to B6 mice.

Experiments were carried out in accordance with the European Communities Council Directive of November 24, 1986 (86/609/EEC). All efforts were made to minimize both the suffering and the number of animals used.

**The Real-Time Ionophoretic TMA Method.** The ECS diffusion parameters (i.e.,  $\alpha$ ,  $ADC_{TMA}$ , and  $k'$ ) were measured by using the real-time ionophoretic method, as described in refs. 14 and 18. In summary, TMA (a substance to which cell membranes are relatively impermeable) was released by ionophoresis from a micropipette, and its local concentration was measured with TMA<sup>+</sup> ion-selective microelectrodes (ISMs) located  $\approx 100$ – $150$   $\mu\text{m}$  from the release site (see Fig. 1a). Ionophoretic electrodes were made from theta-glass tubing (Clark Electromedical Instruments, Pangbourne, U.K.) and filled with 150 mM TMA<sup>+</sup>. The concentration of TMA<sup>+</sup> was then measured by means of a double-barreled TMA<sup>+</sup>-ISM at a fixed distance from the tip of the ionophoretic electrode. TMA<sup>+</sup> ISMs were prepared by a procedure described in ref. 18. We used a Corning 477317 ion exchanger, and the ion-sensitive barrel was back-filled with 150 mM TMA<sup>+</sup> chloride. The reference barrel contained 150 mM NaCl. The shank of the ionophoretic electrode was bent so that it could be aligned parallel to the TMA<sup>+</sup> ISM. The bent ionophoresis microelectrode and ISM were then glued together in a fixed array, and the spacing of the tips was measured before and after each experiment by using a microscope equipped with a graticule. The time-dependent rise and fall of the extracellular TMA<sup>+</sup> concentration during and after an ionophoretic pulse (TMA<sup>+</sup> diffusion curves; Fig. 1b) were fitted to a radial diffusion equation modified to account for extracellular volume fraction  $\alpha$ , the  $ADC_{TMA}$ , and the nonspecific TMA<sup>+</sup> uptake  $k'$  (14). Diffusion curves were first recorded in 0.3% agar gel in 150 mM NaCl/3 mM KCl/1 mM TMA chloride to calibrate the microelectrode array (in agar  $\alpha = 1$ ,  $k' = 0$  and  $ADC_{TMA} = 1,043 \mu\text{m}^2\text{s}^{-1}$ ; free diffusion coefficient, 25°C). Similar recordings repeated in layers III–VI of the cerebral cortex were analyzed to yield the ECS diffusion parameters  $\alpha$ ,  $ADC_{TMA}$ , and  $k'$ . Measurements of ECS diffusion parameters were performed at several depths (in 100- $\mu\text{m}$  steps from a depth of 200–300  $\mu\text{m}$  to 600–900  $\mu\text{m}$  below the brain surface) in one to three tracks (70 tracks in 39 animals) within the somatosensory cortex (1.5 mm posterior to bregma, 1.5 mm lateral to midline). All measurements within one track were averaged, and the averages were used for final statistics.

Animals were anesthetized with sodium pentobarbital (initial dose, 90 mg/kg; dose each subsequent 1 h, 30 mg/kg). Their cortex was exposed by 1-mm-diameter trephination holes (1.5 mm lateral and either at bregma or 1.5 mm caudal to bregma), and the dura was removed from this area. During measurements, the animals were placed in a stereotaxic apparatus (David Kopf Instruments, Tujunga, CA). The body temperature was maintained at 37°C, and breathing was spontaneous.

**DW-MRI.** DW-MRI measurements were performed by using an experimental magnetic resonance (MR) spectrometer Biospec 4.7 T system (Bruker, Ettlingen, Germany) equipped with a 200 mT/m gradient system and a head surface coil. For diffusion-weighted measurements, four coronal slices were selected (thickness, 0.8 mm;

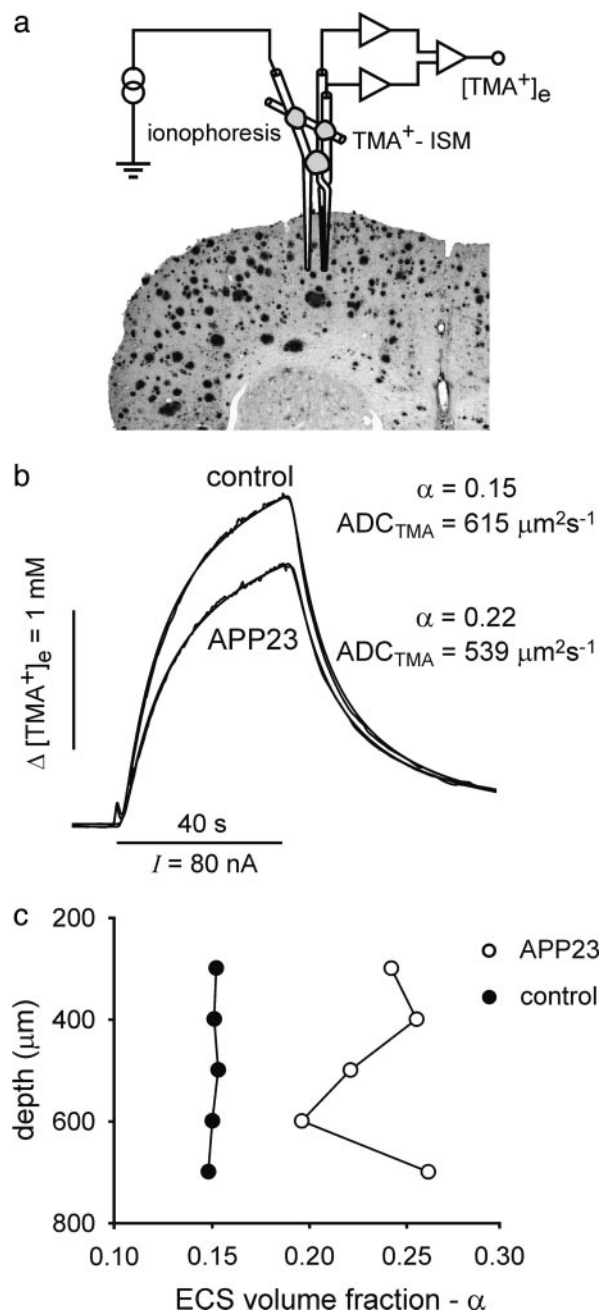


**Fig. 1.** TMA<sup>+</sup> measurements and typical diffusion curves in control and APP23 mice. (a) A double-barreled TMA<sup>+</sup>-selective microelectrode (TMA<sup>+</sup> ISM) and a micropipette for TMA<sup>+</sup> iontophoresis were glued together with dental cement to stabilize the intertip distance at 100–150  $\mu\text{m}$ , and this microelectrode array was introduced into the dorsal brain cortex. (b) Comparison of TMA<sup>+</sup> diffusion curves obtained in 17- to 25-month-old transgenic and control mice. The diffusion parameters can be determined from the shape and magnitude of the curves. The ECS was larger, and  $ADC_{TMA}$  was lower, in APP23 animals than in controls. (c) ECS volume fraction ( $\alpha$ ) plotted against the depth of measurements (the zero level corresponds to the brain surface);  $\alpha$  was changed in 17- to 25-month-old APP23 mice compared with age-matched controls.

interslice distance, 1.2 mm; field of view,  $1.92 \times 1.92 \text{ cm}^2$ ; matrix size,  $256 \times 128$ ). DW images were measured by using the stimulated echo sequence and the following parameters: b-factors, 136, 329, 675, 1,035, 1,481, and 1,825  $\text{s}/\text{mm}^2$ ;  $\Delta = 30 \text{ ms}$ ; echo time, 46 ms; repetition time, 1.2 s. The diffusion gradient pointed along the

**Table 1. ECS volume fraction ( $\alpha$ ), ADC<sub>TMA</sub>, and ADC<sub>W</sub> in control and APP23 mice**

Diffusion parameters	Control females		Control males		APP23 females		APP23 males	
	6–8 months old	17–25 months old	6–8 months old	17–25 months old	6–8 months old	17–25 months old	6–8 months old	17–25 months old
$\alpha$	0.199 ± 0.006	0.132 ± 0.006*†	0.203 ± 0.006	0.161 ± 0.008*	0.194 ± 0.009	0.226 ± 0.011**	0.187 ± 0.007	0.218 ± 0.010**
ADC <sub>TMA</sub> , $\mu\text{m}^2\text{s}^{-1}$	608 ± 30 (n = 6, N = 4)	609 ± 17 (n = 11, N = 7)	585 ± 17 (n = 5, N = 3)	590 ± 12 (n = 12, N = 7)	599 ± 9 (n = 7, N = 4)	557 ± 15 <sup>†</sup> (n = 13, N = 6)	587 ± 16 (n = 6, N = 3)	577 ± 9 (n = 10, N = 5)
ADC <sub>W</sub> , $\mu\text{m}^2\text{s}^{-1}$	602 ± 10 (N = 6)	547 ± 8*† (N = 7)	591 ± 11 (N = 3)	594 ± 9 (N = 6)	597 ± 15 (N = 8)	574 ± 9 <sup>‡</sup> (N = 8)	596 ± 7 (N = 4)	589 ± 3 (N = 7)

N, number of animals; n, number of measurements (microelectrode tracks). Data are given as mean ± SEM.

\* $P < 0.05$ , between 6- to 8-month-old mice and 17- to 25-month-old mice of the same group, as determined by two-tailed Mann–Whitney  $t$  test.

<sup>†</sup>Gender-based significant differences within control and APP23 groups.

<sup>‡</sup>Significant differences detected between APP23 mice and age- and gender-matched controls.

rostrocaudal direction. Maps of ADC<sub>W</sub> were calculated by using the linear least-squares method. ADC<sub>W</sub> was assumed to be zero in pixels where the acquired data did not fit well to theoretical dependence (correlation coefficient was  $< 0.2$ ). These zero-values were ignored for statistical evaluation if they occurred in the region of interest (ROI). ADC<sub>W</sub> maps were analyzed by using IMAGEJ software (W. Rasband, National Institutes of Health, Bethesda). The evaluated ROIs were positioned by using a mouse brain atlas (19) in both the left and right hemispheres. The minimal area of an individual ROI was 1.2 mm<sup>2</sup>. In each animal, we analyzed four coronal slices from the interval between 0.8 mm frontal to bregma and 3.6 mm caudal to bregma. The resulting eight values of ADC<sub>W</sub> (two ROIs per slice, four slices) were averaged to obtain a single representative value for comparison with other mice.

The quality of ADC<sub>W</sub> measurements was verified by means of five diffusion phantoms placed on the top of a mouse's head. The phantoms were made from glass tubes (inner diameter, 2.3 mm; KS80 glass, Růckl Glass, Otovice, Czech Republic) filled with pure (99%) substances having different diffusion coefficients. We used the following substances: 1-octanol, *n*-undecane (Sigma–Aldrich), isopropyl alcohol, 1-butanol, and *tert*-butanol (Penta, Prague). The temperature of the phantoms was maintained at a constant 37°C. The average diffusion coefficient for each compound was determined at the same time as the experimental measurements of each group of mice and compared with the average diffusion coefficient of the same compound measured in conjunction with the measurements of the other groups of mice.

ADC<sub>W</sub> was measured in the same animals in which the TMA measurements were performed 1 week later. For MRI measurements, the animals were anesthetized with isoflurane (1.5% in a gas mixture of 35% O<sub>2</sub>/65% N<sub>2</sub>O) administered by a face mask. The mice were placed in a heated cradle, and their heads were fitted in a built-in head holder (Rapid Biomedical, Rimpär, Germany).

**Behavioral Testing.** The ability to cognitively process spatial information was tested in a Morris water maze (20). A computerized tracking system (21) had been used previously. In the Morris-water-maze task, the animals were trained to localize an invisible escape platform hidden below the water surface in a large pool. The pool had a diameter of 80 cm and was located in an experimental room rich in natural environmental cues (for e.g., doors and windows). The escape platform had a diameter of 11 cm and was positioned 5 mm under the water surface in the center of a quadrant of the pool. The animals were given 60 s to find the platform in each search trial. If the mice failed to find a platform within the time limit, they were guided to reach it by the experimenter. The next search was started  $\approx 25$  min later. The training program lasted 9 days, and the animals made four searches every day. Escape latencies were measured during training procedures; asymptotic escape latencies were taken as an average of the escape latencies of three consecutive trainings at days 7–9. An additional probe trial was performed on day 6. In the probe trials, the escape platform was removed, and

the animals were allowed to swim freely for 60 s in the pool. The number of crossings over the former position of the target (annuli crossings) was calculated and compared with the number of annuli crossings over symmetrical locations in the other three quadrants. All of the animals were tested for the visual-placing reaction to eliminate any mice with vision deficits that may affect performance in the water maze.

**Histology and Analysis of Amyloid Load.** Immediately after TMA diffusion measurements, the animals, under deep anesthesia, were perfused transcardially with 0.1 M PBS (pH 7.4), followed by buffered 4% paraformaldehyde (pH 7.4). Brains were removed and postfixed (24 h) in the same fixative. Then, they were stepwise dehydrated in 10%, 20%, and 30% sucrose solutions. After freezing, 25- $\mu\text{m}$  serial coronal sections were cut on a freezing-sliding microtome and collected in 0.1 M Tris-buffered saline (pH 7.4). Immunohistochemistry was done according to published protocols (22) by using the NT12 polyclonal antibody directed against amyloid  $\beta$ .

Amyloid load was assessed on every 20th section throughout the neocortex immunostained with NT12. The percentage of neocortical volume occupied by amyloid (amyloid load) was determined by sampling through the entire neocortex and calculating the percentage of points from a superimposed point grid that touched amyloid (23). Stereological analysis was performed with the aid of STEREOLOGE software (Systems Planning and Analysis, Lanham, MD).

**Statistical Analysis.** All data are presented as mean ± SEM. The differences between groups were evaluated by using the Mann–Whitney nonparametric two-tailed test (INSTAT, GraphPad, San Diego). ANOVA was done with STATISTICA software (StatSoft, Tulsa, OK). The differences were considered significant at  $P < 0.05$ .  $N$  and  $n$  indicate the number of mice and the number of measurements, respectively.

## Results

**TMA<sup>+</sup> Diffusion Measurements.** ECS diffusion parameters were studied in eight distinct groups of animals (6- to 8-month-old and 17- to 25-month-old control and APP23 mice). Males and females were evaluated separately. A comparison of ECS volume fraction  $\alpha$ , the ADC<sub>TMA</sub>, and nonspecific uptake  $k'$  in the cortex of 6- to 8-month-old APP23 transgenic and 6- to 8-month-old control mice revealed no significant differences. The values of volume fraction  $\alpha$  and ADC<sub>TMA</sub> values are summarized in Table 1. The results obtained in control and transgenic mice were within the range of values found previously in the rodent cortex (24, 25). Diffusion measurements were performed in cortical layers III–VI. No significant differences between individual cortical layers were found; however, in layer VI, there was a slight decrease in ADC<sub>TMA</sub>.

In 17- to 25-month-old controls, the ECS volume fraction was significantly decreased compared with 6- to 8-month-old control mice (Table 1). This 25% decrease was quite uniform, with no

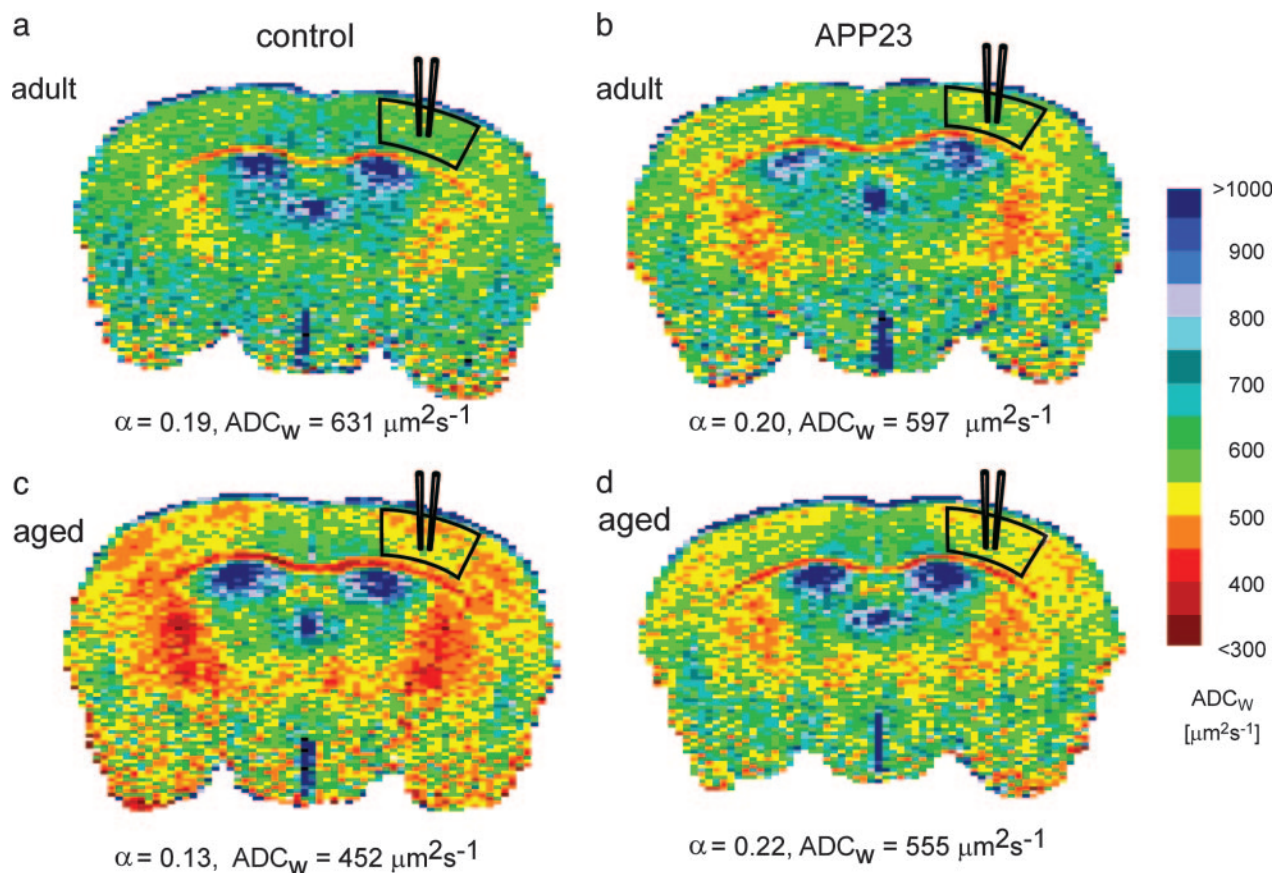


**Fig. 2.**  $ADC_w$  maps acquired in the brain of control and APP23 female mice. The mean value of  $ADC_w$  was calculated in the areas indicated. In the corresponding region, TMA<sup>+</sup> measurements were performed on the same animals a few days later. The mean values of  $ADC_w$  and ECS volume fraction ( $\alpha$ ) are given below each map. There were no differences between adult control (a) and adult transgenic (b) mice. (a and c) A decrease in  $ADC_w$  and  $\alpha$  was found during aging in control mice. In aged APP23 mice (d), there was an increase in both  $ADC_w$  and  $\alpha$  when compared with age-matched control mice (c).

differences observed between individual cortical layers. Interestingly, the decrease was more pronounced in females, with  $\alpha$  being significantly lower in aged females than in aged males ( $P = 0.0095$ ).

In both male and female 17- to 25-month-old APP23 mice, the ECS volume fraction increased significantly in comparison with both their age-matched controls and also adult (6- to 8-month-old) control animals.  $ADC_{TMA}$  significantly decreased only in 17- to 25-month-old APP23 females when compared with age-matched controls. Typical diffusion curves are shown in Fig. 1*b*. Fig. 1*c* shows the typical variations of ECS volume fraction at different depths in the cortex of an APP23 aged female compared with the uniform values in a control aged female. The larger amplitude of the diffusion curve in Fig. 1*b* indicates a smaller ECS volume fraction, whereas the slower increase and decrease of the diffusion curves reflects a lower  $ADC_{TMA}$ . Nonspecific TMA<sup>+</sup> uptake was significantly higher in both control and APP23 aged groups [ $k' = (5.0 \pm 0.4) \times 10^{-3} \text{ s}^{-1}$ ] compared with the respective groups of 6- to 8-month-old animals [ $k' = (3.0 \pm 0.5) \times 10^{-3} \text{ s}^{-1}$ ].

**MR Measurements of  $ADC_w$ .**  $ADC_w$  maps of coronal brain slices were evaluated in the primary somatosensory cortex in the location that corresponded to the site of TMA measurements (see Fig. 2). Details about the evaluation of  $ADC_w$  maps are given in *Materials and Methods*. Fig. 2 shows typical  $ADC_w$  maps measured in female mice. To visualize the differences between animals,  $ADC_w$  maps were converted to pseudocolor images.

During aging,  $ADC_w$  decreased significantly in control female mice (Fig. 2*a* and *c*). We compared the mean values of  $ADC_w$  in the somatosensory cortex of APP23 transgenic mice with those

measured in age-matched controls. In 6- to 8-month-old transgenic APP23 animals, the values of  $ADC_w$  were not significantly different from controls (Fig. 2*b*). Female 17- to 25-month-old APP23 mice showed a higher  $ADC_w$  than age-matched controls (Fig. 2*d*). In males, we did not observe significant differences in  $ADC_w$  between young and aged animals or between APP23 mice and controls.

The differences in diffusion coefficients between any two individual measurements of the phantoms were <5%, and there were no significant differences in the diffusion coefficients of the same compound measured in conjunction with different groups of mice. These findings demonstrate the good reproducibility of our  $ADC_w$  measurements and confirm that no systematic errors occurred.

**Behavioral Testing.** The main results of the behavioral tests are summarized by the learning curves shown in Fig. 3*a* and *b*. Two-way ANOVA (8 groups  $\times$  9 days) with repeated measures on days revealed significant main effects of groups ( $F_{7,34} = 5.91, P < 0.01$ ) and days ( $F_{8,272} = 60.02, P < 0.01$ ) as well as significant interaction ( $F_{56,272} = 1.46, P < 0.05$ ). Newman-Keuls post hoc tests showed that all groups except the old transgenic females decreased their escape latencies from 35–55 s on day 1 to asymptotic values of 7–17 s on days 7–9. The aged APP23 females started to differ from the other groups on day 4 ( $P < 0.05$ ) and continued to perform poorly until the end of the experiment ( $P < 0.01$ ).

In the probe-trial experiment, the old female transgenic mice showed no preference for the target quadrant and made fewer crossings of the target annulus than the mice of the other age-matched groups (Fig. 3*c*). These groups, as well as all of the adult

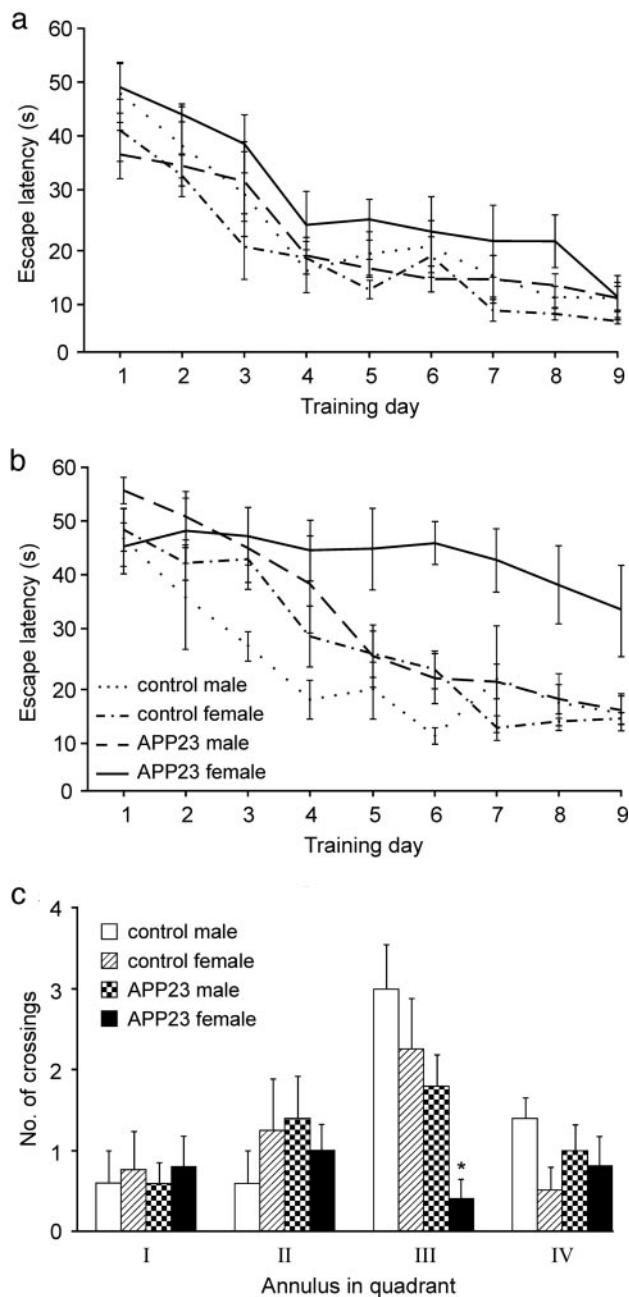


**Fig. 3.** Results of behavioral testing of control and APP23 mice. (a) Adult mice. (b) Aged mice. (a and b) No between-group differences in learning performance could be demonstrated on days 1 or 2. The escape latencies of the old female transgenic mice started to differ significantly from the other groups on day 3, and their performance did not improve throughout the duration of the experiment. However, learning of the old male transgenic mice did not differ from their respective controls. (c) Aged mice. In the probe trial on training day 6, the old female transgenic mice showed no preference for the target quadrant, made fewer annuli crossings, and visited the target position significantly less frequently than the other groups.

mouse groups, clearly preferred the target quadrant and especially the area corresponding to the target location, and there were no significant differences among the groups.

**The  $\beta$ -Amyloid Plaque Load.** Histological sections stained for amyloid plaque load were analyzed in the cortex of 6- to 25-month-old APP23 mice. The plaque load increased with the increasing age of

the animals. In 6- to 8-month-old mice, the amyloid plaque load was  $<1.6\%$  in both males and females. In animals older than 17 months, the amyloid plaque load was significantly higher in females ( $20.0 \pm 1.6\%$ ,  $n = 13$ ) than in males ( $10.4 \pm 2.5\%$ ,  $n = 8$ ). However, the amyloid plaque load varied greatly (in females, the plaque load ranged 9–26%; in males, the plaque load ranged 3–18%).

## Discussion

The concentration of  $\beta$ -amyloid is one of the key factors in its transition from a monomeric to a fibrous form and its aggregation into amyloid plaques (26). The  $\beta$ -amyloid concentration can be influenced substantially by changes in interstitial fluid diffusion and bulk flow in the perivascular spaces (27). In our study, we investigated extracellular diffusion in the cerebral cortex of transgenic APP23 mice and age-matched controls. The following two age groups were selected: adult 6- to 8-month-old mice that were just starting to develop amyloid plaques, and old 17- to 25-month-old mice with a mean amyloid plaque load of 15.2%.

The values of the ECS diffusion parameters obtained in 6- to 8-month-old control animals did not significantly differ from published data (11, 15, 16). In age-matched APP23 mice, we did not detect any significant differences. This observation would imply that the ECS diffusion parameters are not changed substantially in young animals before amyloid deposition.

Aging in control mice was associated with a decrease in ECS size, in agreement with our previous measurements in aged rats (13, 28). Our study shows that the decrease found in the mice is even more pronounced than it is in rats and, furthermore, that it is greater in aged females than in males. The decrease in ECS volume fraction during aging might be attributed to the loss of extracellular matrix molecules such as chondroitin sulfate proteoglycans (CSPG), fibronectin (13), or highly sialylated cell-adhesion molecules, such as polysialic acid neural cell-adhesion molecule (NCAM) (29). Recently, we found that in knock-out mice lacking tenascin-R (a glycoprotein that is an important component of the extracellular matrix), the ECS is significantly smaller than in wild-type mice (30). Therefore, extracellular matrix molecules may act like a sponge by binding a large number of water molecules, and because of the mutual repulsion of their numerous negatively charged residues, they tend to occupy a lot of space. Thus, their loss during aging might lead to a decrease in the ECS volume. ECS shrinkage might also be related to a general decrease in hydration during aging. Dehydration is associated with an increase in colloid density (31), resulting in a decrease in catalytic enzyme activity and possibly contributing to the accumulation and deposition of certain substances intracellularly and extracellularly. In particular, the decrease in ECS volume during aging might contribute to the early stages of amyloid plaque formation.

Also, we have found a significant difference in the ECS volume fraction between aged control females and age-matched control males. An even more pronounced difference was found for  $ADC_w$ . This sex difference is probably the first observation of a gender difference in these two parameters. However, other differences have been described by Mouton *et al.* (32), who reported that female mice have a greater number of astrocytes and microglia in the hippocampus than males and that this difference increases with age. Mouton *et al.* suggested that these changes might be related to the decrease in 17 $\beta$ -estradiol after estropause; however, there is no direct evidence. In aged APP23 mice, we found a significant increase in ECS volume fraction and a decrease in the  $ADC_{TMA}$ , closely related to plaque deposition. The simplest explanation is that the extracellular deposition of amyloid directly results in ECS enlargement, representing at the same time an additional diffusion barrier and, thus, leading to a decrease in  $ADC_{TMA}$ . An alternative explanation could be that an increased concentration of soluble amyloid attracts water into the ECS.

Unlike TMA, water crosses cell membranes relatively easily; for that reason,  $ADC_w$  does not characterize only the diffusion prop-

erties of the ECS but also the diffusion properties of the intracellular space and the permeability of cell membranes for water (33). Our MRI measurements revealed that  $ADC_W$  changes in APP23 mice predominantly corresponded to variations in ECS volume. In the cortex of aged animals, there was no significant difference in  $ADC_{TMA}$  among the measured groups of animals, although  $ADC_W$  decreased. This result could be related to the fact that  $ADC_W$  is composed of many components (34, 35). In contrast to the TMA method, which measures  $ADC_{TMA}$  exclusively in the ECS, the MR method measures a weighted average  $ADC_W$  across multiple subcompartments that differ in their diffusion properties, e.g., in the extracellular and intracellular spaces. If the volume ratio between the subcompartments changes in the tissue, then the resulting  $ADC_W$  is affected also (30).

Is there a link among ECS volume, diffusion changes, and the behavioral deficits that we have found in aged female APP23 mice? A similar gender-dependent impairment of water-maze performance in aged APP23 mice (36) was attributed to the observation that the plaque load was three times higher in females than in males (37). In the experiments that we describe here, the plaque load was only 1.9 times higher in females than in males, but the behavioral deficit was well expressed. This observation suggests that the navigation failure observed in aged female APP23 mice could not only be due to the accumulation of amyloid plaques but also to concomitant changes in ECS volume and other diffusion parameters, which may contribute to a decrease in the extracellular concentration of many important neuroactive substances, such as acetylcholine, dopamine and serotonin, and to a decreased efficiency of volume transmission. The functional radius of protein and peptide molecules, including hormones and growth factors, would also be compromised. An increase in ECS volume leads to diminished extracellular-field potentials and reduced excitability in the

neocortex (38). Glutamate and  $\gamma$ -aminobutyric acid spillover and crosstalk between synapses, which depend critically on diffusion parameters, have been suggested to play a role in long-term potentiation and long-term depression (39, 40). Therefore, the changes in ECS volume and  $ADC_{TMA}$  observed in our study, the rearrangement of astrocytic processes, and amyloid plaques can contribute to behavioral deficits in severely affected APP23 females.

The volume of the ECS measured by the TMA method is only that part of the ECS that is available for the diffusion of  $TMA^+$ . Obviously, the volume of amyloid plaques, which are located extracellularly, is not included in the ECS volume fraction as measured by the TMA method. The amyloid plaque load in old female transgenic mice is  $\approx 20\%$  (i.e., one-fifth of the tissue volume is occupied by amyloid). The real ECS volume is the sum of both these volumes; in old female transgenic mice, it is  $\approx 40\%$  of the tissue volume. The possible consequences are cell shrinkage/death and/or the loss of their processes because of the greatly reduced intracellular compartment. Because the only way that neurons and glial cells can communicate is by extracellular diffusion, we can expect changes in neuron–glia interactions, synaptic efficacy, and synaptic plasticity (16, 17, 41) in the APP23 mouse model of Alzheimer's disease.

We thank Matthias Staufenbiel (Novartis Pharma, Basel) from Novartis Pharma for providing us with both APP23 transgenic mice and the wild-type animals. We also thank Prof. Charles Nicholson for his careful reading of an earlier version of this article and for providing suggestions that have increased the clarity of our presentation. This work was supported by Academy of Sciences of the Czech Republic Grants AVOZ5039906 and LN00A65 and Ministry of Education, Youth and Sports of the Czech Republic Grant J13/98111300004.

- Selkoe D. J. (2001) *Physiol. Rev.* **81**, 741–766.
- Glenner, G. G. & Wong, C. W. (1984) *Biochem. Biophys. Res. Commun.* **120**, 885–890.
- Masters, C. L., Multhaup, G., Simm, G., Pottgiesser, J., Martins, R. N. & Beyreuther, K. (1985) *EMBO J.* **4**, 2757–2763.
- Kang, J., Lemaire, H. G., Unterbeck, A., Salbaum, J. M., Masters, C. L., Grzeschik, K. H., Multhaup, G., Beyreuther, K. & Muller-Hill, B. (1987) *Nature* **325**, 733–736.
- Sturchler-Pierrat, C., Abramowski, D., Duke, M., Wiederhold, K. H., Mistl, C., Rothacher, S., Ledermann, B., Burki, K., Frey, P., Paganetti, P. A., et al. (1997) *Proc. Natl. Acad. Sci. USA* **94**, 13287–13292.
- Meyer-Luehmann, M., Stalder, M., Herzog, M. C., Kaeser, S. A., Kohler, E., Pfeifer, M., Boncristiano, S., Mathews, P. M., Mercken, M., Abramowski, D., et al. (2003) *Nat. Neurosci.* **6**, 370–377.
- Syková, E., Mazel, T., Vargová, L., Voříšek, I. & Prokopová-Kubinová, S. (2000) *Prog. Brain Res.* **125**, 155–178.
- Syková, E. (2003) *Isr. J. Chem.* **43**, 55–69.
- Fuxe, K. & Agnati, L. F. (1991) *Volume Transmission in the Brain* (Raven, New York).
- Zoli, M., Jansson, A., Syková, E., Agnati, L. F. & Fuxe, K. (1999) *Trends Pharmacol. Sci.* **20**, 142–150.
- Syková, E. (1997) *Neuroscientist* **3**, 28–41.
- Voříšek, I. & Syková, E. (1997) *J. Cereb. Blood Flow Metab.* **17**, 191–203.
- Syková, E., Mazel, T., Hasenöhr, R. U., Harvey, A. R., Šimonová, Z., Mulders, W. H. & Huston, J. P. (2002) *Hippocampus* **12**, 269–279.
- Nicholson, C. & Phillips, J. M. (1981) *J. Physiol. (London)* **321**, 225–257.
- Nicholson, C. & Syková, E. (1998) *Trends Neurosci.* **21**, 207–215.
- Syková, E. (2004) *Neurochem. Int.* **45**, 453–466.
- Syková, E., *Neuroscience*, in press.
- Syková, E., Svoboda, J., Polák, J. & Chvátal, A. (1994) *J. Cereb. Blood Flow Metab.* **14**, 301–311.
- Franklin, K. B. J. & Paxinos, G. (1997) *The Mouse Brain in Stereotaxic Coordinates* (Academic, San Diego).
- Morris, R. J. (1984) *J. Neurosci. Methods* **11**, 47–60.
- Kaminsky, Y. & Krekule, I. (1997) *Physiol. Res.* **46**, 223–231.
- Stalder, M., Phinney, A., Probst, A., Sommer, B., Staufenbiel, M. & Jucker, M. (1999) *Am. J. Pathol.* **154**, 1673–1684.
- Calhoun, M. E., Wiederhold, K. H., Abramowski, D., Phinney, A. L., Probst, A., Sturchler-Pierrat, C., Staufenbiel, M., Sommer, B. & Jucker, M. (1998) *Nature* **395**, 755–756.
- Voříšek, I., Hájek, M., Tintěra, J., Nicolay, K. & Syková, E. (2002) *Magnet. Reson. Med.* **48**, 994–1003.
- Syková, E., Fiala, J., Antonova, T. & Voříšek, I. (2001) *Eur. J. Pediatr. Surg.* **11**, S34–S37.
- Westlind-Danielsson, A. & Arnerup, G. (2001) *Biochemistry* **40**, 14736–14743.
- Weller, R. O., Massey, A., Newman, T. A., Hutchings, M., Kuo, Y. M. & Roher, A. E. (1998) *Am. J. Pathol.* **153**, 725–733.
- Syková, E., Mazel, T. & Šimonová, Z. (1998) *Exp. Gerontol.* **33**, 837–851.
- Abrous, D. N., Montaron, M. F., Petry, K. G., Rougon, G., Darnaudery, M., Le Moal, M. & Mayo, W. (1997) *Brain Res.* **744**, 285–292.
- Voříšek, I., Antonova, T., Mazel, T., Hájek, M. & Syková, E. (2003) *Proc. Intl. Soc. Mag. Reson. Med.* **11**, 1983.
- Van der Sanden, M. J. T., Nagy, K., Semsei, I. & Zs-Nagy, I. (1995) *Arch. Gerontol. Geriatr.* **20**, 273–282.
- Mouton, P. R., Long, J. M., Lei, D. L., Howard, V., Jucker, M., Calhoun, M. E. & Ingram, D. K. (2002) *Brain Res.* **956**, 30–35.
- Gass, A., Niendorf, T. & Hirsch, J. G. (2001) *J. Neurol. Sci.* **186**, S15–S23.
- Pfeuffer, J., Provencher, S. W. & Gruetter, R. (1999) *MAGMA* **8**, 98–108.
- Weglarz, W. P., Adamek, D., Markiewicz, J., Skorka, T., Kulinowski P. & Jasinski, A. (2004) *Solid State Nucl. Magn. Reson.* **25**, 88–93.
- Kelly, P. H., Bondolfi, L., Hunziker, D., Schlecht, H.-P., Carver, K., Maguire, E., Abramowski, D., Wiederhold, K.-H., Sturchler-Pierrot, O., Jucker, M., et al. (2003) *Neurobiol. Aging* **24**, 365–378.
- Callahan, M. J., Lipinski, W. J., Feng, B., Durham, R. A., Pack, A. & Walker, L. C. (2001) *Am. J. Pathol.* **158**, 1173–1177.
- Kume-Kick, J., Mazel, T., Voříšek, I., Hrabětová, S., Tao, L. & Nicholson, C. (2002) *J. Physiol.* **542**, 515–527.
- Piet, R., Vargová, L., Syková, E., Poulain, D. A. & Oliet, S. H. R. (2004) *Proc. Natl. Acad. Sci. USA* **101**, 2151–2155.
- Min, M. Y., Asztely, F., Kokaia, M. & Kullmann, D. M. (1998) *Proc. Natl. Acad. Sci. USA* **95**, 4702–4707.
- Araque, A., Carmignoto, G. & Haydon, P. G. (2001) *Annu. Rev. Physiol.* **63**, 795–813.